

Green Synthesis and Characterization of ZnO- Ag Nanocomposite by *Thymus vulgaris*

Mina Zare^{1,2}, K. Namratha^{1,2}, K.Byrappa^{1,2} *

¹DOS in Earth Science, Mansagangothri, University of Mysore, Mysore, India

²Centre for Materials Science and Technology, Vijnana Bhavana, University of Mysore, Mysore, India

*Corresponding author: kbyrappa@gmail.com

ABSTRACT

In this study, ZnO-Ag nanocomposite (NCs) was synthesized less than 20 nm through a simple and eco-friendly bio-hydrothermal method by using aqueous *Thymus vulgaris* (Thyme) leaf extract. Thyme leaf extract was used as a reducing agent and surfactant in the green synthesis of ZnO-Ag NCs. Crystal structure, Functional group, morphology, chemical elemental, the band gap of ZnO-Ag NCs were characterized by using powder X-ray diffraction, Fourier Transform Infrared Spectroscopy, Transmission Electron Microscopy, Energy Dispersive X-ray analysis, UV-visible spectroscopy, respectively. TEM results confirmed the size and morphology of nanocomposite. The influence of silver nitrate concentration in the formation of ZnO-Ag NCs was studied. This study future aims that to use biocompatible ZnO-Ag nanocomposite for biological application and food packaging.

Keywords: Hydrothermal synthesis, Thyme leaf extract, ZnO-Ag Nanocomposite, Characterization

I. INTRODUCTION

Metal and metal oxide nanoparticles are interesting because of their great optical, chemical, electrical and magnetic properties [1]. These properties bring the materials interesting in different application areas, including nanoelectronics devices, catalysis, nonlinear optical devices, bio-medical, etc [2]. Metal oxides semiconductor nanocomposites have been widely explored due to their potential applications in various fields [3].

Between metal and metal oxides, Ag and ZnO nanoparticles have attracted large attention, not only because ZnO has great chemical stability, low cost, large surface area and wide-band gap with various applications, including use in electronics, solar cells,

photo electronics and sensors, but also because Ag nanomaterials illustrate some unique features in biological and chemical sensing and high electrical conductivity. Additionally, Ag modification is found to be effective for the synthesis of p-type ZnO, as the naturally occurring ZnO demonstrates n-type conductivity as a result of its innate defects such as oxygen vacancies and zinc interstitials [4]. Recently, Ag ions become more attractive of the several research works, due to their novel effects on the evolution of antibacterial activity and efficiency of photocatalytic activity of semiconductor [5].

On the other hand, recently zinc oxide nanoparticles have received much consideration due to it has a vast range of attributes that depend on doping, with a range of conductivity from metallic to

insulating (consist of p-type and n-type conductivity), piezoelectricity, room-temperature ferromagnetism, large band gap (3.37 eV at 300 K), high transparency, wide binding energy (60 meV), semi-conductivity, high melting point $\sim 1975^{\circ}\text{C}$, chemical-sensing effects and huge magneto-optic [6]. ZnO nanoparticles have been synthesized with numerous morphologies in the nanoregime, such as belts [6], rods [7], prisms [8], flowers [9], rings [10] and many more. Various methods that have been used to fabricate Ag/ZnO NCs include hydrothermal synthesis [11], template-confined synthesis routes [12], Solvothermal method [13] and microwave heating and sonochemical method [14].

In the present article, Ag-ZnO NCs with 2 nm diameters of Ag particles via facile bio-hydrothermal method was reported. Impact of Thyme leaf extract and incorporation of Ag into ZnO crystal on their structural, optical properties are studied in details. The synthesized ZnO-Ag NCs illustrate great crystallinity of ZnO-Ag NCs.

II. METHODS AND MATERIAL

Thyme leaf was picked up from Nandi hills attached to Chamundi Hill, Mysore, India. The analytical grade of all chemicals was used in the preparation of samples in this work and was used as received. Silver nitrate (N/10, Rankem, India), NaOH (99%, Sigma-Aldrich, India), $\text{Zn}(\text{NO}_3)_2 \cdot 6\text{H}_2\text{O}$ (99%, Alfa Aesar, India), ethanol (99%, Alfa Aesar, India). Deionized water (DI water, ELGA, PURELAB Option Q7, $18.2 \text{ M}\Omega \text{ cm}$) was used during the studies.

The synthesis of ZnO NPs with aqueous Thyme extract was reported earlier by same authors. ZnO-Ag NCs was manufactured with slight modification involving single step bio-hydrothermal synthesis. In this study the best concentration of previously reported articles was considered as a basic and silver nitrate volume was altered to fabricate ZnO-Ag NCs. General purpose autoclaves made of

stainless steel (SS316), provided with teflon liners of 30 ml capacity were used for the synthesis of ZnO-Ag NCs. Silver nitrate (10/N), Zinc nitrate (1 M) and sodium hydroxide (10 M) solution with different volume were prepared and mixed under the stirring condition for 30 minutes. 0.5 ml Thyme leaf extract was added to 11.5 ml of all above solutions and sonicated for 45 minutes. 12 ml of the solution was transferred to the teflon liner and placed in an autoclave. The autoclave was kept in a hot air oven for 4 hours at 150°C . Then cooled down to room temperature and washed with double distilled water and ethanol several times by centrifuging at 7000 rpm for 15 min. The precipitate was collected and kept for drying at 50°C for 24 hours. Samples were collected for further characterization and analysis.

The crystalline behaviour and structural properties of the products were identified by powder X-ray diffraction (PXRD) with $\text{CuK}\alpha 1$ ($\lambda = 1.542 \text{ \AA}$) radiation in the range of (2θ) from 20 to 80°C at room temperature (Rigaku Smart Lab, Automated Multipurpose X-ray diffractometer, Japan). Transmission electron microscope (TEM, Jeol/JEM 2100 model, USA, operating at 200 kV) and energy dispersive X-ray spectrometer (EDX) were carried out to characterize the morphologies, size and chemical elements. The UV-Vis spectroscopy was measured by SA 165 Diode array spectrophotometers to determine the band gap. Fourier transform infrared (FT-IR) spectrophotometer was analysed with a JASCO FTIR-460 plus spectrophotometer, Japan, using KBr wafers in the range of $400\text{-}4000 \text{ cm}^{-1}$ to analyse the surface chemistry of NCs.

III. RESULTS AND DISCUSSION

XRD patterns of the as-synthesized ZnO-Ag NCs were revealed by powder X-ray diffraction measurement. Figure 1 illustrates the XRD pattern of ZnO-Ag NCs, bare ZnO NPs and Ag NPs. The peaks in the XRD pattern shows the face-center-cubic (fcc)

metallic structure of Ag (JCPDS card no. 04-0783) and hexagonal wurtzite structure of ZnO (JCPDS card no. 36-1451). For Ag nanoparticles, the main characteristic peaks at 2θ values 37.2, 44.6 and 64.5, which belonged to the (111), (200), (220) planes of fcc, approve the formation of Ag nanoparticles [15]. With adding the Ag content there is a slight shift of Ag peaks to lower 2θ angles due to the substitution of Ag^+ ions for Zn^{2+} in the ZnO lattice. The XRD peaks for ZnO–Ag demonstrate the formation of clear, distinct phases for both Ag and ZnO. Formation of distinct phases for both ZnO and Ag in the ZnO–Ag is revealing the fabrication of crystalline nanocomposite. The identified peaks represent the purity of nanocomposite [16].

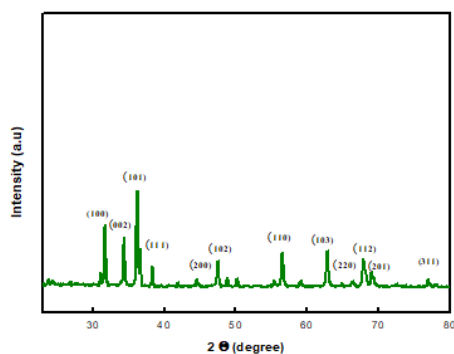


Figure 1: PXRD patterns of ZnO–Ag NCs, ZnO NPs and Ag NPs

The typical IR spectrum of ZnO NPs, ZnO–Ag NCs and Thyme leaf extract are given in Figure 2. FTIR spectra of NCs exhibited prominent peaks at 458, 1380 and 3450 cm^{-1} . The strong absorption peak at 460 cm^{-1} is attributed to Zn–O stretching vibration of the ZnO NPs [17]. The intensity of ZnO peak reduced after formation of Ag NPs on the surface of ZnO NPs [33-34]. The spectral band at 1384 cm^{-1} corresponds to the symmetric stretching of acetate species [20]. The existence of broad band at 3449 cm^{-1} corresponds to the stretching vibration of the O–H mode. This may be owing to the hydroxyl groups of water [16]. The absorption peak in Thyme leaf extract at 1041 belong to C–N stretching in primary amine [15]. The small

peak at 1615 cm^{-1} is attributed to the O–H bending mode due to adsorption of water molecules [21]. Thyme leaf extract contains polyphenolic compounds that major constituents are thymol, isothymol, followed by monoterpenes, linalool and α -terpnoeol [22].

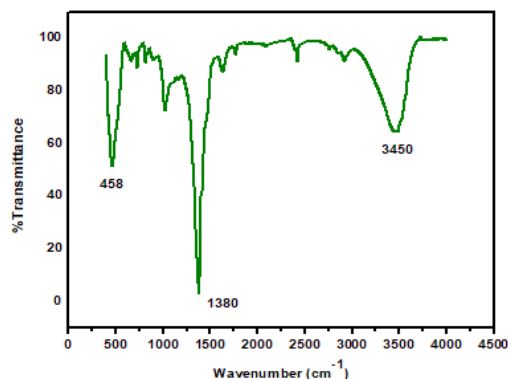


Figure 2: FTIR spectra of ZnO–Ag

Figure 3a depicts the morphology and size of as synthesized ZnO–Ag NCs using TEM which displays the formation of ~ 20 nm spherical Ag nanoparticles on the surface of ZnO particles. NCs were obvious from TEM images. The size of NCs shows less than 20 nm. **Figure 3b** demonstrates the corresponding EDS pattern. The result displays there aren't other impurities in EDX profile. The EDS findings visibly signify the presence of Zn, Ag and O in the synthesized NCs. The elemental analysis by EDS represents 30.74, 15.90 and 53.36 weight percentage of NCs is for Zn, Ag and O respectively.

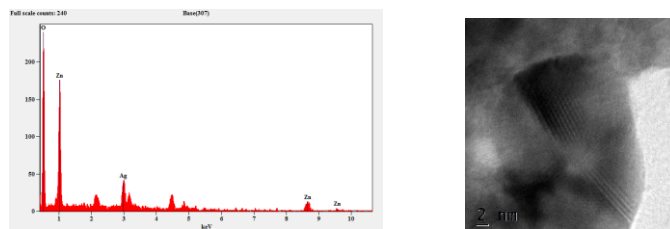


Figure 3 a: HRTEM image showing lattice fringes of both ZnO and Ag, 3b: EDAX spectrum obtained from SEM for ZnO–Ag NCs

The optical absorption of ZnO–Ag NCs at room temperature was evaluated by UV–Vis spectroscopy.

Figure 4 shows the UV visible spectroscopy of as prepared samples and pristine ZnO. The UV-Vis spectrum of ZnO-Ag NCs exhibited a maximum absorption peak at 381 nm, while the bulk ZnO displayed a peak at 373 nm. The band gap of bulk ZnO and ZnO-Ag NCs found to be 3.32 eV and 3.25 eV respectively. The presence of Ag NPs improves the band gap absorption in comparison to the bare ZnO NPs [23]. Ag NPs work function ranges in between the valence band (VB) and conduction band (CB) of ZnO NPs that accelerates the light absorption capacity [24].

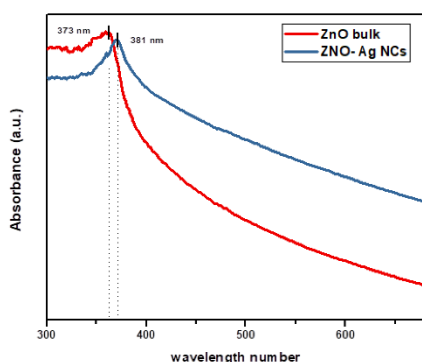


Figure 4: UV-vis absorption spectrum of bulk ZnO-Ag NCs and bulk ZnO

IV. CONCLUSION

To conclude, the present study established a facile eco-friendly method to produce ZnO-Ag NCs through a bio-hydrothermal method using Thyme leaf extract. Characterizations accomplish using XRD, FTIR, UV-Visible, TEM, EDS confirm the formation of ZnO-Ag NCs. However, biological studies are mandatory to assess the potential cytotoxicity, biosafety and biocompatibility of such nanomaterials in vitro as well as in vivo.

V. REFERENCES

- [1] I. Khan, K. Saeed, and I. Khan, Nanoparticles: Properties, applications and toxicities, Arab. J. Chem., 2017.
- [2] X.-F. Zhang, Z.-G. Liu, W. Shen, and S. Gurunathan, (2016.). Silver Nanoparticles: Synthesis, Characterization, Properties, Applications, and Therapeutic Approaches. *Int. J. Mol. Sci.*, 17 (9): p. 1534.
- [3] R. Sahay, V. J. Reddy, and S. Ramakrishna, (2014). Synthesis and applications of multifunctional composite nanomaterials, 9:25.
- [4] S. Ghosh, V. S. Goudar, K. G. Padmalekha, S. V. Bhat, S. S. Indi, and H. N. Vasan, (2012). ZnO/Ag nanohybrid: synthesis, characterization, synergistic antibacterial activity and its mechanism, *RSC Adv.*, 2 (3): p. 930–940.
- [5] T. Ghosh, A. B. Das, B. Jena, and C. Pradhan, (2015). Antimicrobial effect of silver zinc oxide (Ag-ZnO) nanocomposite particles, *Front. Life Sci.*, 8 (1):p. 47–54.
- [6] Z. Fan and J. G. Lu, (2005). Zinc oxide nanostructures: synthesis and properties. *J. Nanosci. Nanotechnol.* 5 (10): p. 1561–1573.
- [7] K. J. I. K. Lee, Study of Stability of ZnO Nanoparticles and Growth Mechanisms of Colloidal ZnO Nanorods, 2005.
- [8] R. Marsalek, (2005). Particle Size and Zeta Potential of ZnO, *APCBEE Procedia.* (9): p. 13–17.
- [9] A. Hezam et al., (2017). Heterogeneous growth mechanism of ZnO nanostructures and the effects of their morphology on optical and photocatalytic properties, *CrystEngComm.* 19 (24): p. 3299–3312.
- [10] S. H, Manikandan, B. Ahmed M, G. V, and G. V, (2017). Enhanced Bioactivity of Ag/ZnO Nanorods-A Comparative Antibacterial Study (Sbds), *J. Nanomed. Nanotechnol.* 4(3): p. 1–7.
- [11] K. Byrappa and M. Yoshimura, *Hydrothermal Technology—Principles and Applications.* 2001.
- [12] H. Zhang, X. Ma, J. Xu, J. Niu, and D. Yang, (2003). Arrays of ZnO nanowires fabricated by

- a simple chemical solution route, *Nanotechnology*, 14 (4): p. 423–426.
- [13] Y. Zheng, L. Zheng, Y. Zhan, X. Lin, Q. Zheng, and K. Wei, (2007). Ag/ZnO Heterostructure Nanocrystals: Synthesis, Characterization, and Photocatalysis, *Inorg. Chem.* 46 (17): p. 6980–6986.
- [14] S. C. Motshekga, S. S. Ray, M. S. Onyango, and M. N. B. (2013). Momba, Microwave-assisted synthesis, characterization and antibacterial activity of Ag/ZnO nanoparticles supported bentonite clay, *J. Hazard. Mater.* (262): p. 439–446.
- [15] M. S. Jadhav, S. Kulkarni, P. Raikar, D. A. Barretto, S. K. Vootla, and U. S. Raikar, (2018). Green biosynthesis of CuO & Ag–CuO nanoparticles from *Malus domestica* leaf extract and evaluation of antibacterial, antioxidant and DNA cleavage activities, *New J. Chem.* 42 (1): p. 204–213.
- [16] R. Zamiri et al., (2014). Far-infrared optical constants of ZnO and ZnO/Ag nanostructures, *RSC Adv.* 4 (40): p. 20902–20908.
- [17] S. Aiswarya Devi, M. Harshiny, S. Udaykumar, P. Gopinath, and M. Matheswaran, (2017). Strategy of metal iron doping and green-mediated ZnO nanoparticles: dissolubility, antibacterial and cytotoxic traits, *Toxicol. Res. (Camb)*. 6 (6): p. 854–865.
- [18] R. Zamiri et al., (2014). Far-infrared optical constants of ZnO and ZnO/Ag nanostructures, *RSC Adv.*, 4 (40): p. 20902–20908.
- [19] P. Devaraj, P. Kumari, C. Aarti, and A. Renganathan, (2013). Synthesis and Characterization of Silver Nanoparticles Using Cannonball Leaves and Their Cytotoxic Activity against MCF-7 Cell Line, *J. Nanotechnol.* (2013): p. 1–5.
- [20] K. Saoud, R. Alsoubaihi, N. Bensalah, T. Bora, M. Bertino, and J. Dutta, (2015). Synthesis of supported silver nano-spheres on zinc oxide nanorods for visible light photocatalytic applications, *Mater. Res. Bull.*, (63): p. 134–140.
- [21] M. Zare, K. Namratha, K. Byrappa, D. M. Surendra, S. Yallappa, and B. Hungund, Surfactant Assisted Solvothermal Synthesis of ZnO Nanoparticles and Study of their Antimicrobial and Antioxidant Properties, *J. Mater. Sci. Technol.*, 2017.
- [22] T. Ibrahim, H. Alayan, and Y. Al Mowaqet, (2012). The effect of Thyme leaves extract on corrosion of mild steel in HCl, *Prog. Org. Coatings.* 75 (4): p. 456–462.
- [23] S. Adhikari, A. Banerjee, N. K. Eswar, D. Sarkar, and G. Madras, (2015). Photocatalytic inactivation of *E. coli* by ZnO–Ag nanoparticles under solar radiation, *RSC Adv.*, 5 (63): p. 51067–51077.
- [24] Y. Li, X. Zhao, and W. Fan, (2011). Structural, Electronic, and Optical Properties of Ag-Doped ZnO Nanowires: First Principles Study, *J. Phys. Chem. C*, 115 (9): p. 3552–3557.